

Nanocolumnar Preferentially Oriented PSZT Thin Films Deposited on Thermally Grown Silicon Dioxide

S. Sriram · M. Bhaskaran · A. Mitchell ·
D. R. G. Mitchell · G. Kostovski

Received: 24 July 2008 / Accepted: 22 October 2008 / Published online: 11 November 2008
© to the authors 2008

Abstract We report the first instance of deposition of preferentially oriented, nanocrystalline, and nanocolumnar strontium-doped lead zirconate titanate (PSZT) ferroelectric thin films directly on thermal silicon dioxide. No intermediate seed or activation layers were used between PSZT and silicon dioxide. The deposited thin films have been characterised using a combination of diffraction and microscopy techniques.

Keywords PSZT thin films · Silicon dioxide · Nanocrystal · XRD · Microscopy

Introduction

There is potential for harnessing the nonlinear properties of ferroelectric thin films for applications in photonics and integration with left-handed materials (metamaterials), as has been demonstrated for bulk ferroelectric crystals [1, 2]. These applications demand that ferroelectric thin films are deposited on dielectric and optically transparent material. One of the most suitable dielectric layers for the deposition of ferroelectrics is silicon dioxide (SiO_2), considering its thermal stability and suitability for optical applications.

Lead zirconate titanate (PZT) is most commonly used ferroelectric material in commercial applications and results of characterisation of PZT thin films have been extensively reported (e.g. [3, 4]). While deposition of thin films on PZT on SiO_2 has been investigated [5, 6], attaining perovskite structured *c*-axis (columnar) growth directly on SiO_2 has proved to be a challenge. Excellent approaches using intermediate layers to seed or control the subsequent PZT deposition have been proposed [5, 6]. While these result in *c*-axis oriented PZT films, the use of seed layers demands additional deposition steps and access to materials. Most importantly, we have observed that an additional layer needs to be incorporated into models used to simulate nonlinear characteristics for thin films.

In this work, we demonstrate that we have overcome this need for intermediary seed layers, in the deposition of columnar PZT compounds on SiO_2 , using optimised deposition conditions. We report on the growth of perovskite structured nanocolumnar strontium-doped PZT (PSZT) thin films. We have used strontium-doped PZT, rather than undoped PZT, in order to capitalise on its enhanced ferroelectric and piezoelectric properties [7–9], which in turn will influence its electro-optic performance.

Experimental Details

Deposition of PSZT Thin Films

PSZT thin films were deposited by RF magnetron sputtering under conditions listed in Table 1. The PSZT thin films had a composition corresponding to 1.6% A-site strontium doping of PZT, with a 65:35 zirconium-titanium ratio. Deposition was carried out on (100) silicon substrates with 300 nm of silicon dioxide grown by thermal

S. Sriram (✉) · M. Bhaskaran · A. Mitchell · G. Kostovski
Microelectronics and Materials Technology Centre, School of
Electrical and Computer Engineering, RMIT University,
GPO Box 2476V, Melbourne, VIC 3001, Australia
e-mail: sharath.sriram@gmail.com

D. R. G. Mitchell
Institute of Materials Engineering, Australian Nuclear Science
and Technology Organisation, PMB 1, Menai, NSW 2234,
Australia

Table 1 PSZT thin film deposition conditions

Target	$(\text{Pb}_{0.92}\text{Sr}_{0.08})(\text{Zr}_{0.65}\text{Ti}_{0.35})\text{O}_3$
Target diameter	100 mm
RF power	100 W
Target to substrate distance	70 mm
Process gas	10% oxygen in argon
Base pressure	9.0×10^{-6} Torr
Sputtering pressure	1.0×10^{-2} Torr

oxidation. Thin film deposition was carried out for 3 h at a process pressure of 10 mTorr which was found to be most suitable to attain desired thin film composition [10]. The films were found to be 750–800 nm thick using an Ambios XP-2 surface profilometer, corresponding to a deposition rate of 250–267 nm/h.

For obtaining films exhibiting suitable ferroelectric properties, thermal processing was carried out (either post-deposition or in situ). The aim of this processing was to enable crystal growth in the thin films and attain *c*-axis orientation.

PSZT thin films were deposited either at room temperature followed by an annealing process or at a substrate temperature of 700 °C. PSZT thin films deposited at room temperature were subject to post-deposition furnace annealing at 700 °C for 3 h in the presence of high purity argon. In the case of samples deposited at temperatures of 700 °C, the samples were heated to deposition substrate temperature at a ramp rate of 10 °C/min and cooled, subsequent to deposition, at 5 °C/min; previous work has shown that these conditions improve the degree of perovskite orientation in the thin films [11].

X-ray Diffraction Analysis

PSZT thin film samples were cleaned by rinsing in solvents (acetone and isopropyl alcohol) and deionised water. Glancing angle X-ray diffraction (XRD) analysis was carried out using a Scintag X-ray diffractometer with an X-ray incidence angle of 5°. The data presented correspond to radiation from copper $K\alpha$ wavelength.

Atomic Force Microscopy Analysis

The surface roughness and grain sizes of the PSZT thin films were studied using atomic force microscopy (AFM). AFM scans were carried out using a Digital Instruments Dimension 3100 scanning probe microscope with a Nanoscope IIIa controller. The scans were carried out in contact mode.

Electron Microscopy Analysis

Cross-section analysis of the thin films was carried out on a field emission gun scanning electron microscope (FEI Nova NanoSEM). Plan view specimens for transmission electron microscopy (TEM) analysis were prepared by mechanically grinding away the backing silicon from the film. The specimens were then ion milled to electron transparency at room temperature using 4 kV argon ions incident at 5°. The analysis was carried out at an accelerating voltage of 200 kV on a JEOL 2010F TEM with a Gatan Imaging Filter.

Results and Discussion

X-ray Diffraction Analysis

The X-ray diffractogram of PSZT thin films deposited at room temperature and subjected to post-deposition annealing is shown in Fig. 1a, and consists of peaks at expected 2θ positions [12]. These peaks are characterised by weak reflections and broad peak widths, indicative of weak preferential orientation, limited grain growth, and a nanocrystalline structure.

Figure 1b is representative of diffractograms obtained for PSZT thin films deposited at substrate temperature of 700 °C. Expected perovskite peaks at 2θ of 29.6° and 49.3°, for (104) and (108) orientations, for a rhombohedral PSZT unit cell [12] were observed. Smaller peaks obtained at 34.3° and 58.5° correspond to (006) and (300) orientations, respectively. The temperature at which these thin films were deposited was chosen to encourage thermally driven grain growth and the diffractogram (Fig. 1b) confirms that this resulted in uniform crystal growth, manifested as strong and sharp peaks in the diffractogram. These results, with strong *c*-axis preference, also promise strong columnar growth in the thin films (discussed in section “[Electron Microscopy Analysis](#)”).

These results indicate that though post-deposition annealing encouraged grain growth, only thin film deposition at high temperatures (in situ substrate heating) results in strong preferential orientation. The PSZT thin film samples deposited at 700 °C, with promising XRD results, were subject to further analyses.

Atomic Force Microscopy Analysis

AFM surface scan results for a PSZT thin film deposited at 700 °C are shown in Fig. 2. The topography images in Fig. 2a, b depicts tightly packed nanocrystalline grains with an average grain size of 80–100 nm. The average surface roughness (R_a) of these films, measured to be about 9–11 nm, indicates that the pronounced grain structure is

Fig. 1 X-ray diffractograms obtained for PSZT thin films: **a** deposited at room temperature with subsequent furnace annealing at 700 °C for 3 h and **b** deposited at a substrate temperature of 700 °C for 3 h

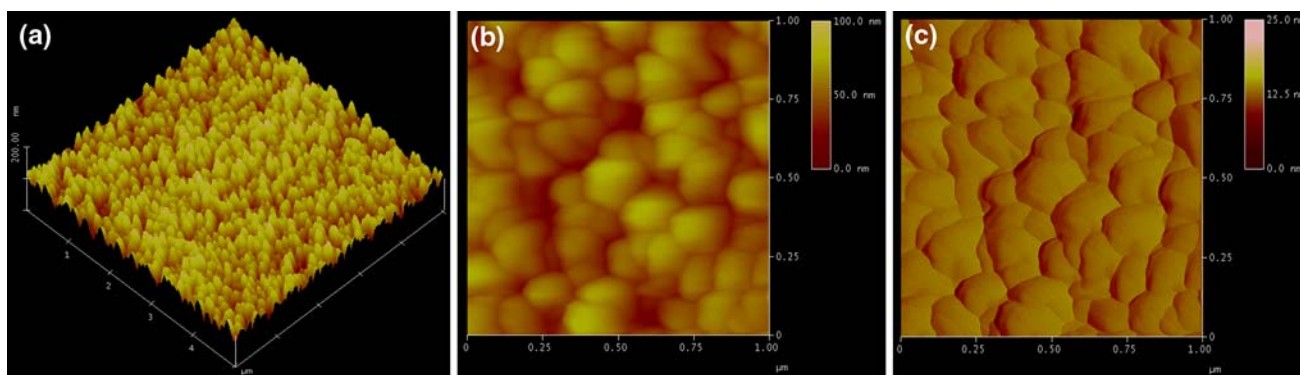
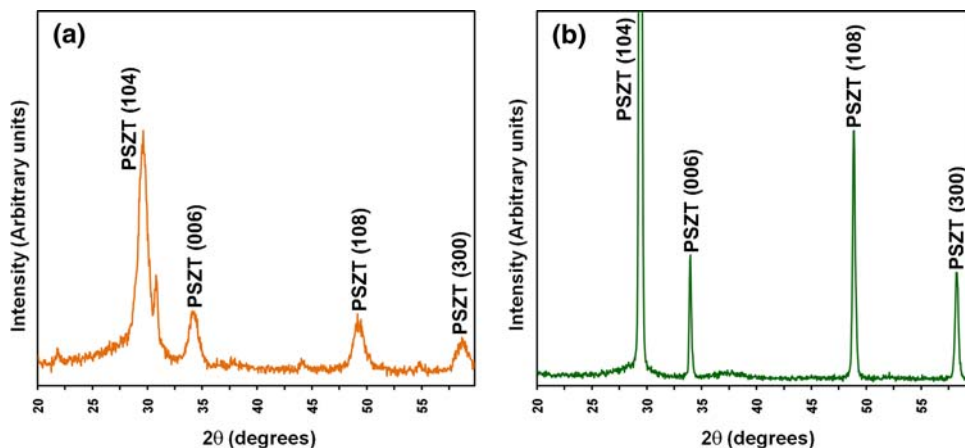
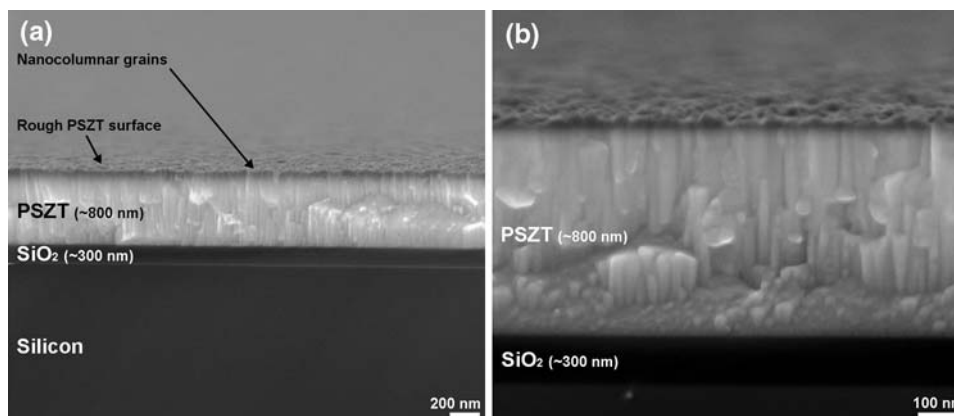


Fig. 2 Atomic force microscopy scan results for PSZT thin film deposited at 700 °C: **a** three-dimensional representation of film surface showing faceted tightly packed grains, **b** topography image

obtained over an area of $1 \times 1 \mu\text{m}^2$, and **c** the deflection image corresponding to the topography in **(b)**

Fig. 3 Cross-sectional scanning electron micrographs in **(a)** and **(b)** showing the regular nanocolumnar grains spanning the thickness of the film (observed at specimen tilt of 9°)



regular. The accentuated faceting of the grain faces is only conveyed by the peak roughness (R_p) values measured to be ~ 90 nm. The polygonal structure of the grains is apparent in the deflection image shown in Fig. 2c.

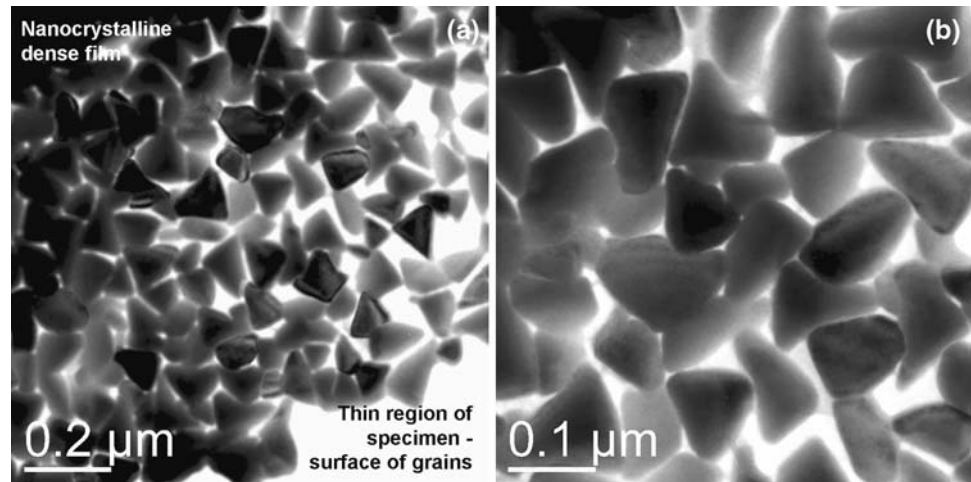
Electron Microscopy Analysis

Cross-sectional scanning electron microscopy (SEM) showed that the films had nanocolumnar grains extending

through the thickness of the PSZT thin films (Fig. 3). The structure and width of these grains matched those expected from XRD and AFM analyses. There are regions where the PSZT grains ends abruptly (especially in Fig. 3b); this was due to the brittle nature of the ceramic PSZT thin films which prevented better sectioning.

Plan view TEM analysis results for PSZT thin films deposited on silicon dioxide are presented in Fig. 4. The nanocrystals observed in the images correspond to grain

Fig. 4 Plan view transmission electron microscopy results obtained for PSZT thin film deposited at 700 °C at two different magnifications are shown in (a) and (b)



sizes of 80–100 nm for the columnar preferentially oriented grains in the structure. A majority of the grains appear to be triangular in shape. AFM scans confirmed that the grains in the PSZT thin film are densely packed, and this can be observed in the top-left of Fig. 4a. In the other region, the ion milling process for the TEM sample preparation has resulted in numerous regions devoid of material. This is a by-product of the very rough crystalline film surface, on which milling from the back results in the majority of the material being removed, with only the capping regions of the grains left behind.

The thin region of the specimen gives us valuable information regarding the nanostructure of the thin films. Figure 4b shows that the grains vary in size from 80 to 100 nm, with well defined crystalline and polygonal structure. Strong Bragg diffraction from many grains in Fig. 4 indicates that they share the same orientation. These nanocrystals extend all the way through the thickness of the specimen forming the columnar structure observed in the cross-sectional analysis. Selected area electron diffraction of the plan view specimen showed that the nanocrystals exhibited the expected perovskite structure, but were randomly distributed—there was no preferential orientation along the substrate surface (XRD indicated preferential orientation perpendicular to the substrate).

A schematic depicting the overall structure of the deposited films is shown in Fig. 5.

Conclusions

This article presents results from the first instance of deposition of preferentially oriented, nanocrystalline, and nanocolumnar PSZT thin films directly on thermal silicon dioxide. No intermediate seed or activation layers were used between PSZT and SiO₂. A substrate temperature of 700 °C was found to be suitable for obtaining the desired

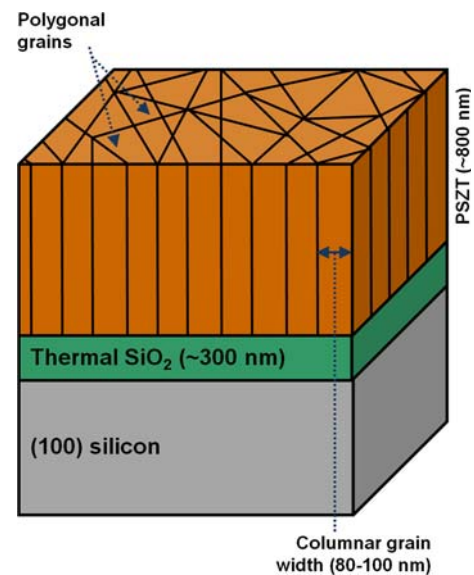


Fig. 5 Schematic representation of the PSZT thin films deposited on thermal SiO₂, showing the nanocolumnar polygonal grain structure (not to scale)

perovskite structure, resulting in films which will exhibit ferroelectric properties suitable for investigation of non-linear properties for photonics and integrated metamaterials applications.

Acknowledgements This research was supported by the Australian Institute of Nuclear Science and Engineering and the CASS Foundation.

References

1. J. Trull, C. Cojocaru, R. Fischer, S.M. Saliel, K. Staliunas, R. Herrero, R. Vilaseca, D.N. Neshev, W. Krolikowski, Y.S. Kivshar, *Opt. Express* **15**, 15868 (2007). doi:10.1364/OE.15.015868
2. R. Fischer, S.M. Saliel, D.N. Neshev, W. Krolikowski, Y.S. Kivshar, *Cent. Eur. J. Phys.* **6**, 569 (2008). doi:10.2478/s11534-008-0073-6

3. P. Muralt, M. Kohli, T. Maeder, A. Kholkin, K. Brooks, N. Setter, R. Luthier, *Sens. Actuators A* **48**, 157 (1995). doi:[10.1016/0924-4247\(95\)00994-9](https://doi.org/10.1016/0924-4247(95)00994-9)
4. Z. Bi, Z. Zhang, P. Fan, *J. Phys. Conf. Ser.* **61**, 120 (2007). doi:[10.1088/1742-6596/61/1/025](https://doi.org/10.1088/1742-6596/61/1/025)
5. J. Zhao, L. Lu, C.V. Thompson, Y. Lu, W.D. Song, *Proc. SPIE* **4426**, 221 (2002). doi:[10.1117/12.456840](https://doi.org/10.1117/12.456840)
6. R. Ramesh, International Patent WO/1994/013471. Available online at <http://www.wipo.int/pctdb/en/wo.jsp?IA=US1993010387>
7. C. Bedoya, C. Muller, J.-L. Baudour, V. Madigou, M. Anne, M. Roubin, *Mater. Sci. Eng. B* **75**, 43 (2000). doi:[10.1016/S0921-5107\(00\)00383-4](https://doi.org/10.1016/S0921-5107(00)00383-4)
8. H. Zheng, I.M. Reaney, W.E. Lee, N. Jones, H. Thomas, *J. Am. Ceram. Soc.* **85**, 207 (2002). doi:[10.1111/j.1151-2916.2002.tb00457.x](https://doi.org/10.1111/j.1151-2916.2002.tb00457.x)
9. S. Sriram, M. Bhaskaran, A.S. Holland, K.T. Short, B.A. Latella, *J. Appl. Phys.* **101**, 104910 (2007). doi:[10.1063/1.2735407](https://doi.org/10.1063/1.2735407)
10. S. Sriram, M. Bhaskaran, J. du Plessis, K.T. Short, V.P. Sivan, A.S. Holland, *Micron* **40**, 104 (2009). doi:[10.1016/j.micron.2007.12.009](https://doi.org/10.1016/j.micron.2007.12.009)
11. S. Sriram, M. Bhaskaran, A.S. Holland, *Semicond. Sci. Technol.* **21**, 1236 (2006). doi:[10.1088/0268-1242/21/9/005](https://doi.org/10.1088/0268-1242/21/9/005)
12. M. Bhaskaran, S. Sriram, D.R.G. Mitchell, K.T. Short, A.S. Holland, *Thin Solid Films* **516**, 8101 (2008). doi:[10.1016/j.tsf.2008.04.041](https://doi.org/10.1016/j.tsf.2008.04.041)